

Exhibit D



Oxidation and degradation of polypropylene transvaginal mesh

Anne D. Talley^a, Bridget R. Rogers^a, Vladimir Iakovlev^{b,c}, Russell F. Dunn^{a,d} and Scott A. Guelcher^{a,e,f}

^aDepartment of Chemical and Biomolecular Engineering, Vanderbilt University, Nashville, TN, USA; ^bLaboratory Medicine and Pathobiology, University of Toronto, Toronto, Canada; ^cDivision of Pathology and Keenan Research Centre of the Li Ka Shing Knowledge Institute, St. Michael's Hospital, Toronto, Canada; ^dPolymer and Chemical Technologies, LLC, Nashville, TN, USA; ^eDepartment of Biomedical Engineering, Vanderbilt University, Nashville, TN, USA; ^fCenter for Bone Biology, Vanderbilt University, Nashville, TN, USA

ABSTRACT

Polypropylene (PP) transvaginal mesh (TVM) repair for stress urinary incontinence (SUI) has shown promising short-term objective cure rates. However, life-altering complications have been associated with the placement of PP mesh for SUI repair. PP degradation as a result of the foreign body reaction (FBR) has been proposed as a contributing factor to mesh complications. We hypothesized that PP oxidizes under *in vitro* conditions simulating the FBR, resulting in degradation of the PP. Three PP mid-urethral slings from two commercial manufacturers were evaluated. Test specimens ($n = 6$) were incubated in oxidative medium for up to 5 weeks. Oxidation was assessed by Fourier Transform Infrared Spectroscopy (FTIR), and degradation was evaluated by scanning electron microscopy (SEM). FTIR spectra of the slings revealed evidence of carbonyl and hydroxyl peaks after 5 weeks of incubation time, providing evidence of oxidation of PP. SEM images at 5 weeks showed evidence of surface degradation, including pitting and flaking. Thus, oxidation and degradation of PP pelvic mesh were evidenced by chemical and physical changes under simulated *in vivo* conditions. To assess changes in PP surface chemistry *in vivo*, fibers were recovered from PP mesh explanted from a single patient without formalin fixation, untreated ($n = 5$) or scraped ($n = 5$) to remove tissue, and analyzed by X-ray photoelectron spectroscopy. Mechanical scraping removed adherent tissue, revealing an underlying layer of oxidized PP. These findings underscore the need for further research into the relative contribution of oxidative degradation to complications associated with PP-based TVM devices in larger cohorts of patients.

ARTICLE HISTORY

Received 11 November 2016
Accepted 3 January 2017

KEYWORDS

Degradation; oxidation;
polypropylene; transvaginal
mesh

Introduction

Surgical treatment options for stress urinary incontinence (SUI) and pelvic organ prolapse (POP) include reconstruction of connective tissue with biological or synthetic grafts. The

CONTACT Scott A. Guelcher Scott.guelcher@vanderbilt.edu

Supplemental data for this article can be accessed at <http://dx.doi.org/10.1080/09205063.2017.1279045>

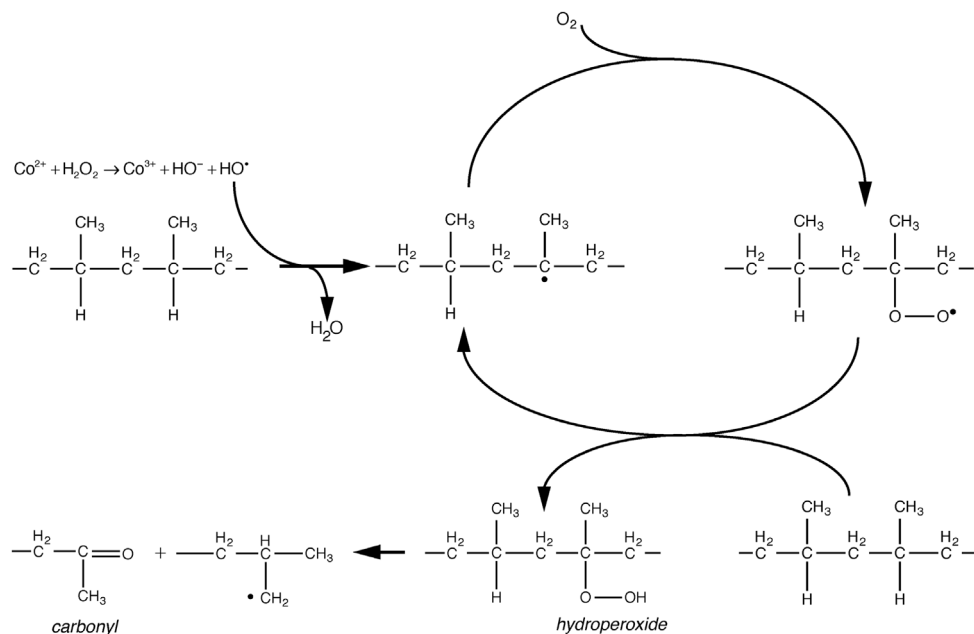


Figure 1. Proposed mechanism of PP oxidation.

most common synthetic grafts are non-resorbable polypropylene (PP) meshes, which have shown promising results in some studies [1,2]. While PP was initially considered inert *in vivo*, despite the fact that it is readily oxidized outside the body [3], its use in transvaginal mesh (TVM) implantations has recently been associated with high complication rates [4–7]. Complications arising from mesh implantation can lead to pain, graft exposure, and specific urinary symptoms [6,8].

Several studies have reported that PP mesh explanted from patients following graft complications revealed evidence of degradation, such as cracking, pitting, and flaking. In the first study explant study, SEM analysis of mesh removed from 100 patients revealed evidence of degradation for the majority of PP monofilament meshes implanted for more than 3 months [9]. In a more recent study, microscopic analysis of 164 explanted TVM devices revealed a layer of degraded PP, which grew thicker with implantation time [10]. Degradation and microcracking of the PP fibers were observed by conventional light microscopy as early as 18 months post-implantation.

Oxidation has been proposed as a potential mechanism of PP degradation *in vivo* [9,11–13]. PP oxidation proceeds through a stable hydroperoxide ($-\text{COOH}$) intermediate prior to chain scission and the formation of a carbonyl ($-\text{C=O}$) end group (Figure 1) [14,15], resulting in a reduction in PP molecular weight, loss of ductility, embrittlement, and crack formation [16]. In a recent study, TVM explanted from 11 patients showed evidence of PP oxidation using FTIR and SEM with X-ray dispersive spectroscopy (SEM/EDS), which distinguished oxidized PP from adsorbed biological material [12]. Oxidation of PP fibers was accompanied by transverse cracking of PP fibers, providing evidence of embrittlement.

Secretion of reactive oxygen species (ROS) by adherent inflammatory cells has been reported to promote oxidative degradation of implanted biomaterials [17–20]. Implantation

Table 1. Physical properties of mid-urethral slings evaluated in this study. All slings are macroporous monofilament Type I meshes with pore sizes >75 µm.

| Product | Abbrev. | Manufacturer | Weight (g m ⁻²) | Pore size (µm) | Filament Size (mm) | Mesh thick- ness (mm) |
|--|---------|-------------------|--------------------------------|----------------|-----------------------|--------------------------|
| Gynecare TVT™ retropubic system | TVT | Ethicon | 105 | 1379 | 0.15 | 0.63 |
| Advantage™ transvaginal Mid-urethral sling system | ADV | Boston Scientific | 100 | 1182 | 0.15 | 0.66 |
| Lynx™ suprapu- bic mid-ure- thral sling system | LYNX | Boston Scientific | 100 | 1182 | 0.15 | 0.66 |

of TVM induces a chronic inflammatory response characterized by adherent macrophages and giant cells that persists for years after implantation [8–10,21]. Recent studies have reported that the foreign body reaction (FBR) is pro-inflammatory, characterized by predominantly M1 macrophages [21] and significantly higher expression of MMP-9 [8]. Furthermore, elevated MMP-9 expression was found to correlate with mesh exposure.

In the present study, we hypothesized that PP mesh oxidizes in response to ROS secreted by adherent inflammatory cells. To test our hypothesis, we investigated the oxidative degradation of three commercial mid-urethral slings (MUSs) *in vitro* using an oxidative medium comprising 20% hydrogen peroxide (H_2O_2) and 0.1 M cobalt chloride ($CoCl_2$), which react to form hydroxyl radicals (OH^{\bullet}) [18,22] that attack the tertiary C–H bond in the PP backbone (Figure 1). This *in vitro* assay recapitulates the oxidative microenvironment between an adherent macrophage and the PP surface [17]. MUS products, which are stabilized with antioxidants to protect against oxidation during high-temperature processing and long-term storage [20], were evaluated to test the hypothesis that the antioxidants do not prevent eventual oxidation and degradation under simulated *in vivo* conditions. Oxidation of PP mesh was measured by Fourier Transform Infrared Spectroscopy (FTIR), and degradation was assessed by Scanning Electron Microscopy (SEM). We also characterized PP mesh fibers explanted from a single patient by X-ray photoelectron spectroscopy (XPS) to analyze PP oxidation *in vivo*. The advantage of the XPS technique is that the composition of atoms and chemical bonds near the surface can be determined, which enables oxidized PP to be differentiated from tissue.

Materials and methods

Materials

Three commercial MUSs were obtained from two device manufacturers: Gynecare TVT™ Retropubic System (Ethicon, Somerset, New Jersey), Advantage™ Transvaginal Mid-Urethral Sling System (Boston Scientific, Marlborough, MA), and Lynx™ Suprapubic Mid-Urethral Sling System (Boston Scientific). All slings are macroporous monofilament Type I meshes with pore sizes >75 µm. Other mesh properties are summarized in Table 1. For the oxidative media, $CoCl_2$ was obtained from Sigma-Aldrich (St Louis, MO) and 30 wt.% H_2O_2 from Fisher Scientific (Pittsburgh, PA).

Table 2. *In vitro* study design.

| Time week | FTIR | | SEM | |
|-----------|-----------|------------------|-----------|------------------|
| | Specimens | Regions/Specimen | Specimens | Regions/Specimen |
| 0 | 3 | 2 | 1 | 5–13 |
| 1 | 3 | 2 | 0 | N/A |
| 3 | 3 | 2 | 0 | N/A |
| 4 | 3 | 2 | 0 | N/A |
| 5 | 3 | 2 | 1 | 7–15 |

In vitro oxidation

For each of the three products listed in Table 1, 17 MUS specimens (approximately 6–7 mg, 1.1 cm by 0.6 cm) were prepared. The study design is listed in Table 2. Thirteen specimens were incubated at 37 °C for up to 5 weeks in oxidative media composed of 0.1 M CoCl₂ in 20 wt.% H₂O₂, which simulates the privileged microenvironment between an adherent macrophage and the PP surface [18–20,22,23]. In this medium, the H₂O₂ and cobalt ions react to form hydroxyl radicals (OH[·], Figure 1) [22]. Samples were submerged by being weighted down using glass beads and were incubated at 37 °C in the oxidative medium on a shaker. At each time point (week 1, 3, 4, or 5), 3 specimens were removed, washed in DI water, and dried. FTIR analysis was performed to test for the presence of hydroxyl (–OH) groups present in the hydroperoxide intermediate and for terminal carbonyl (–C=O) end groups. Two locations on each of the 3 MUS mesh specimens were tested via FTIR, giving *n* = 6 replicates at each time point. At 5 weeks, one specimen was removed, washed in DI water, and dried for SEM analysis to identify evidence of oxidative degradation, such as pitting, flaking, and cracking. The oxidative media was changed every 3–4 days (3). Four pristine mesh specimens (three for FTIR and one for SEM) not incubated in oxidative medium were assessed as the 0-week group.

Fourier transform infrared spectroscopy (FTIR)

FTIR spectra were obtained using a Thermo Electron IR200 spectrometer. FTIR peak areas were quantified using Omnic 8.3 software. The area under the hydroxyl peak was integrated over 3600–3050 cm⁻¹. Carbonyl peaks were integrated from 1750 to 1500 cm⁻¹. For each spectrum, the baseline was manually corrected around the peak of interest in the case of any baseline shifts.

Scanning electron microscopy (SEM)

Meshes were examined for degradation at 5 weeks, since at this time point evidence of significant oxidation was observed in the FTIR spectrum. At 5 weeks, one mesh specimen was removed from oxidative media, dried at room temperature, and sputter-coated for 45 s using a Cressington Q108 sputter coater, which deposited gold at a 30-mA current. One mesh specimen that was not incubated in oxidative medium was imaged as a control (0 weeks group). Specimens were imaged using SEM (Hitachi S-4200 SEM) at a voltage of 1 kV. A total of 5–15 images were taken of each specimen. Images were taken at low (40–150X) and medium (150–1000×) magnification to identify regions of the mesh that showed evidence of degradation. High-magnification images (1000–2000×) were taken of 5-week specimens

to show surface degradation, characterized by flaking (feature size >10 µm), peeling (feature size >10 µm), or pitting (>1 µm deep). These features were not present on control (0 weeks) mesh samples, which showed only specks <1 µm deep, spots, and longitudinal striations on the surface.

X-ray photoelectron spectroscopy (XPS) of explanted PP mesh

After approval of the St. Michael's Hospital Research Ethics Board, an explanted American Medical Systems PP MUS specimen from a single patient, preserved dry without formalin and received by the pathology department at St. Michael's, was selected for testing. The mesh was explanted for complications other than mucosal erosion. A part of the specimen was processed for histology, which showed evidence of a FBR in response to implantation of the mesh with no superimposed acute (bacterial) inflammation. Tissue-free fibers of the PP mesh at the specimen edges were separated from the specimen using ophthalmic tweezers and scissors. To assess the effects of mechanical cleaning on the surface chemistry of the fibers, three distinct regions were characterized by XPS: (1) one area of interest (AOI) on untreated fibers showing no evidence of residual tissue by microscopy (Untreated residue-free group), (2) one AOI on the same untreated fibers showing evidence of residual tissue (Untreated residue-present group), and (3) one AOI on scraped fibers in which the outer layer was mechanically removed using tweezers and a scalpel blade under a dissection microscope (Scraped group). Five Untreated fibers and five Scrapped fibers were analysed by XPS with a PHI Versaprobe using Al $\text{K}\alpha$ x-rays (1486 eV). A 20-µm diameter X-ray spot (AOI) was rastered across the analysis area, and a take-off angle of 45 degrees off sample normal was used. Pass energies of 187.7 and 23.5 eV were used for the survey and high-resolution acquisitions, respectively. Charge neutralization was accomplished using 1.1 eV electrons and 10 eV Ar^+ ions. The energy scales of the high-resolution spectra were calibrated to place $-\text{CH}_2-$ bonding in the carbon 1s spectrum at 284.8 eV. Relative atomic concentrations were calculated using peak areas and handbook sensitivity factors.

Statistical analysis

For each *in vitro* FTIR data-set ($n = 6$) measured for a specific type of mesh at a specific time point, the one-sample Komogorov-Smirnov test failed to reject the null hypothesis that the data-set came from a standard normal distribution ($\alpha < 0.05$). Thus, the data were assumed to be normally distributed. Carbonyl and hydroxyl peak areas were plotted as mean \pm SEM and analyzed using a two-way ANOVA for mesh composition and time. Pairwise comparisons were performed by a Tukey's honestly significant difference (HSD) test.

For each *in vivo* XPS data-set ($n = 5$) measured for a specific surface treatment (Untreated residue-free, Untreated residue-present, and Scraped), the one-sample Komogorov-Smirnov test failed to reject the null hypothesis that the data-set came from a standard normal distribution ($\alpha < 0.05$). Thus, the data were assumed to be normally distributed. Surface atomic concentrations, atomic ratios, and C1s bonding concentrations were plotted as mean \pm SD and analyzed by a one-way ANOVA and Tukey's HSD test for pairwise comparisons. For all FTIR and XPS analysis, the significance level was defined as $p < 0.05$.

Results

In vitro oxidation assessed by FTIR spectroscopy

FTIR spectra taken after 0 weeks immersion time showed minimal hydroxyl (-OH) or carbonyl (-C=O) peaks for each of the PP mesh devices (Figure 2). However, after 5 weeks incubation time, FTIR spectra of all three meshes showed the appearance of both -OH and -C=O groups, which indicates that the PP had oxidized, resulting in the formation of hydroperoxide (-COOH, gray arrow) intermediate and terminal -C=O (black arrow) groups (Figure 2). A two-way ANOVA with Tukey's HSD test for pairwise comparisons showed that the areas of the hydroxyl and carbonyl peaks at 5 weeks were significantly ($p < 0.05$) higher than those at the other time points. No significant differences between the three mesh groups were observed at any time point. These findings confirm our hypothesis that PP mesh oxidizes in response to ROS, such as hydroxyl radicals.

Surface degradation assessed by SEM

Low- (40–60 \times) magnification SEM images at 0 weeks (untreated control, Figure 3(A) top row) and at 5 weeks (Figure 3(B) top row) revealed the knitted monofilament structure of the meshes. Medium- (800–1000 \times) magnification images showed dark spots and longitudinal striations along the axis of extrusion as well as specks $<1\text{ }\mu\text{m}$ deep (Figure 3(A), bottom row). No evidence of features associated with surface degradation was observed, such as flaking ($>10\text{ }\mu\text{m}$ long), peeling ($>10\text{ }\mu\text{m}$ long), or pitting ($>1\text{ }\mu\text{m}$ deep). In contrast, medium-magnification SEM images of PP mesh incubated for 5 weeks in oxidative media (Figure 3(B) middle row) revealed evidence of pits $>1\text{ }\mu\text{m}$ deep (black arrows), peeling flakes $>10\text{ }\mu\text{m}$ long (double white arrows), and shallow craters $>10\text{ }\mu\text{m}$ long (white arrows) on the surface. High- (1500–2000 \times) magnification images showed that small pits $<5\text{ }\mu\text{m}$ in diameter and $>1\text{ }\mu\text{m}$ deep had formed on the surface of the mesh. These pits were observed in all fields of view examined at medium and high magnification. Some regions of the mesh showed evidence of larger scale features, such as detachment of peeling flakes $>10\text{ }\mu\text{m}$ (double white arrows) from the surface, resulting in the formation of shallow craters (white arrows). These observations at 5 weeks are consistent with our hypothesis that PP mesh oxidizes in response to ROS, resulting in PP embrittlement and surface degradation (16).

Oxidation of explanted PP mesh

A survey spectrum was collected from each of the Untreated residue-free, Untreated residue-present, and Scraped AOIs analyzed. An X-ray-induced secondary electron micrograph shows the AOI (white box in Figure 4(A)) analyzed on representative Untreated residue-free and Scraped samples (the complete set of images, spectra, and surface composition data for all groups are presented in the Supplemental Data). A one-way ANOVA with Tukey's HSD test for pairwise comparisons showed no significant ($\alpha < 0.05$) differences in surface atomic concentrations, atomic ratios, or C1s bonding between the residue-free and residue-present AOIs on Untreated fibers. This finding suggests that the AOIs tested are representative of the fiber (within the error of the measurement), since the two AOIs that appeared visibly different showed no significant differences in surface composition. After

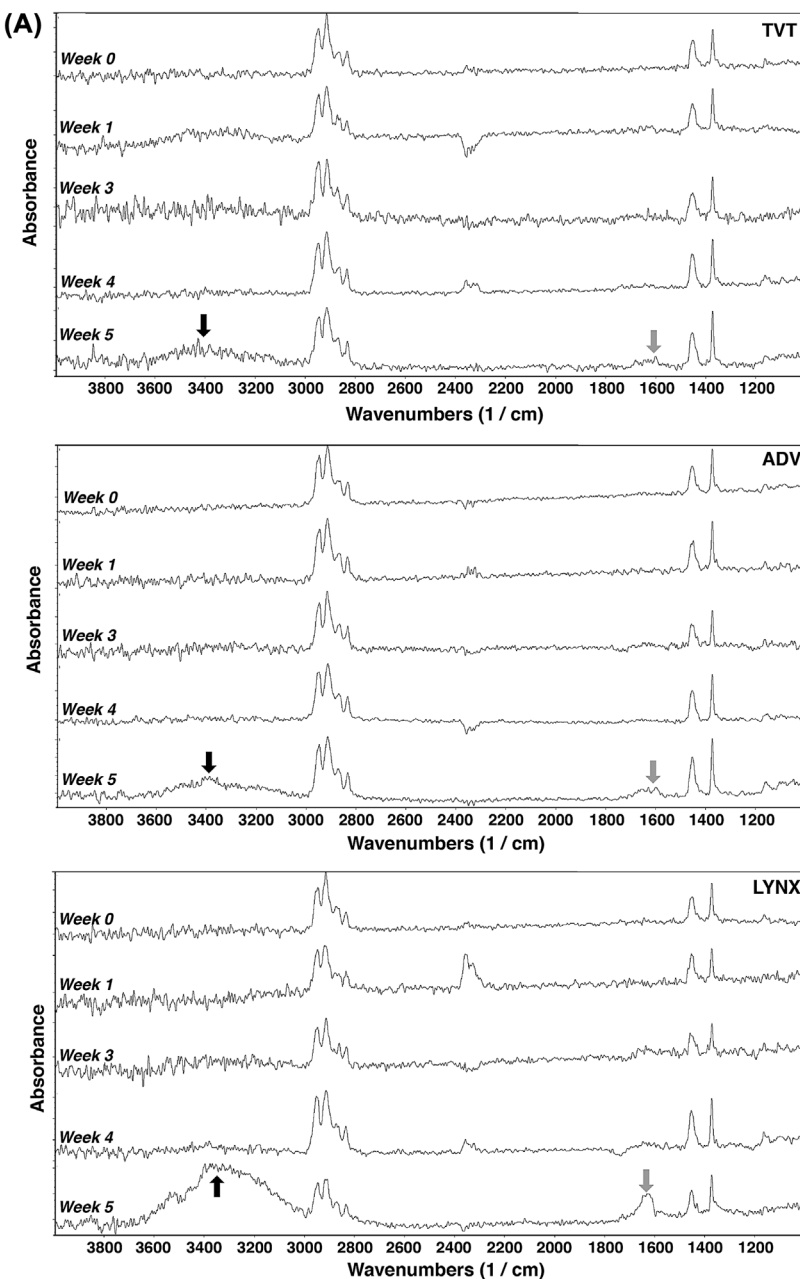
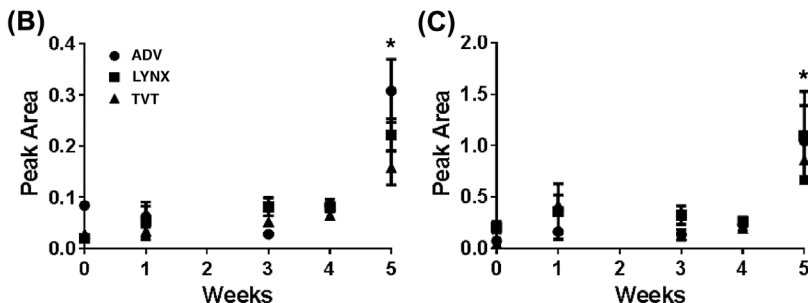


Figure 2. Effects of incubation time in oxidative medium on the composition of PP mesh assessed by FTIR spectroscopy. (A) FTIR spectra of PP mesh samples incubated in oxidative medium for up to 5 weeks at 37 °C. Carbonyl ($-\text{C=O}$, black arrow) and hydroxyl ($-\text{OH}$, gray arrow) peaks increase with time for each mesh. (B–C) Plots of the area of the (B) $-\text{OH}$ peak (integrated over $3600\text{--}3000 \text{ cm}^{-1}$) and (C) $-\text{C=O}$ peaks (integrated over $1750\text{--}1500 \text{ cm}^{-1}$) show a significant increase in carbonyl and hydroxyl peak areas at week 5. Note: *Denotes statistical significance ($p < 0.5$).

**Figure 2.** (Continued).

scraping, the atom-% C significantly increased, the atom-% O significantly decreased, and the atom-% N significantly decreased ($p < 0.05$, Figure 4(B)). Consequently, the atomic ratios O:C, N:C, and N:O significantly decreased after scraping ($p < 0.05$, Figure 4(C)). While all the Untreated samples showed nitrogen on the surface, only one of the Scrapped samples, which were mechanically debrided to remove oxidized PP and protein from the surface, showed nitrogen. In contrast, all of the Scrapped fibers exhibited oxygen on the surface, which is attributed to the presence of residual oxidized PP on the surface after scraping. Thus, mechanical scraping removed adherent tissue to reveal an underlying layer of oxidized PP in this specific patient explant. These findings highlight the potential of XPS analysis of mechanically scraped fibers from explanted mesh without formalin fixation for assessing oxidation of PP mesh *in vivo*.

High-resolution carbon 1s (C1s) spectra from Untreated and Scraped fibers are shown in Figure 4(D). These spectra were curve-fitted to extract the contributions of different carbon bonding configurations present in the spot [24]. All Untreated fibers exhibited some fraction of the carbon present bonded in carbonyl and hydroperoxide configurations. One-way ANOVA with Tukey's HSD test for pairwise comparisons showed that scraping significantly ($\alpha < 0.05$) reduced the percent of C1s bonding configurations comprising carbonyl and hydroperoxide bonds (Figure 4(E)). However, all scraped fibers showed evidence of oxygen on the surface: two showed carbonyl bonding and four showed hydroperoxide bonding. Since nitrogen was observed on the surface of only one scraped fiber, the carbonyl and/or hydroperoxide bonds present on the scraped fibers cannot be attributed to protein adsorption. Thus, the data in Figure 4(D) and (E) reveal evidence of carbonyl and hydroperoxide peaks on Untreated residue-free and Scraped fibers that are consistent with the oxidation reaction mechanism for PP. Explanted mesh from only one patient was evaluated, which precludes statistical analysis of the data to identify differences between patients. However, the XPS findings support our hypothesis that oxidation of PP mesh in response to ROS secreted by adherent inflammatory cells occurred *in vivo* in this specific patient explant.

Discussion

In this study, we hypothesized that PP mesh oxidizes in response to ROS secreted by inflammatory cells that infiltrate the mesh after implantation. To test our hypothesis, we investigated the oxidative degradation of three commercial MUSs using an oxidative medium that recapitulates the microenvironment between adherent macrophages and the PP surface [17].

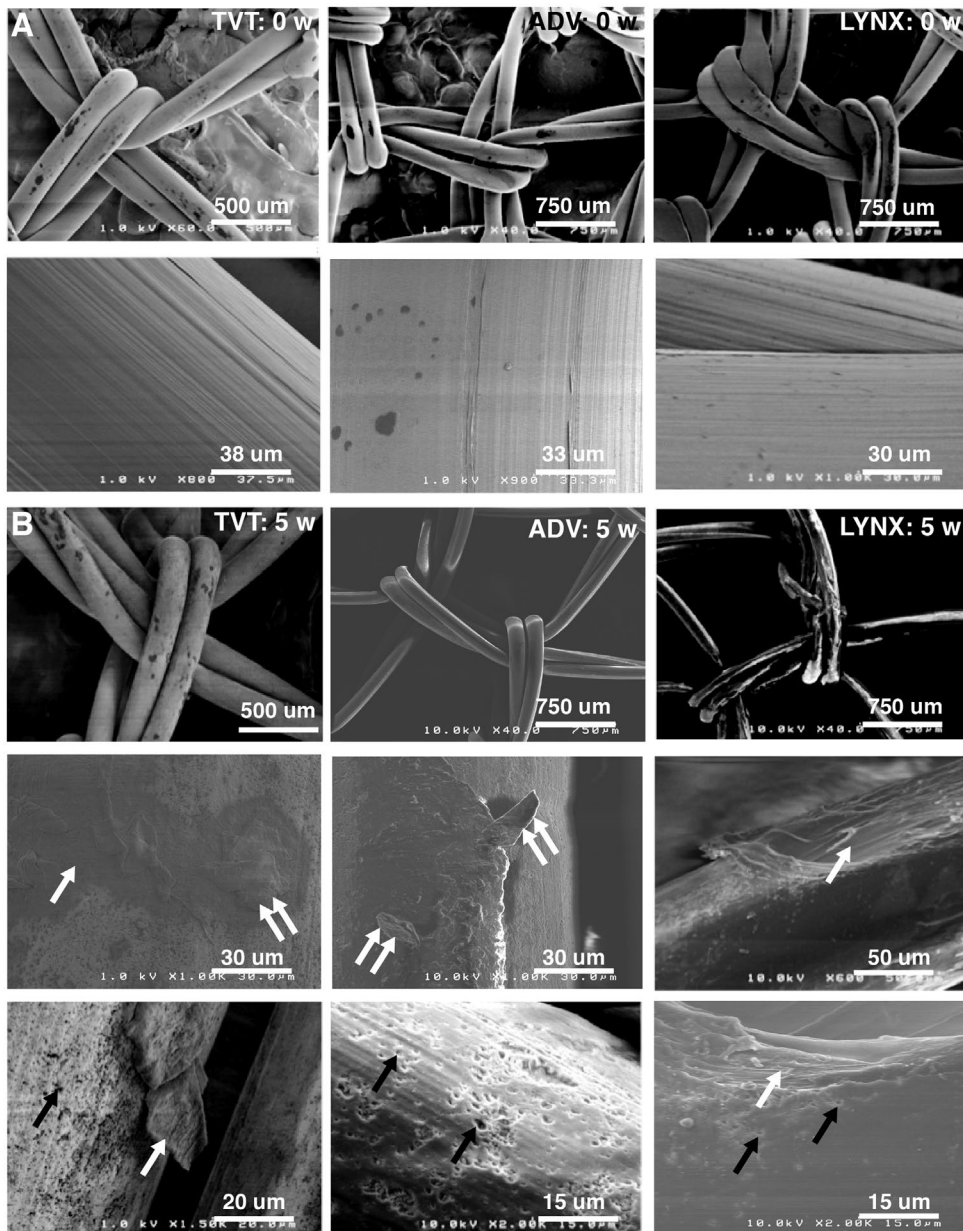


Figure 3. SEM images of PP mesh before and after incubation in oxidative medium. (A) SEM images of pristine TTV, ADV, and LYNX meshes (0 weeks incubation time). Low-magnification (40–60 \times , top row) images show the knitted monofilament structure of the meshes. Medium-magnification (800–1000 \times , bottom row) images show dark spots and longitudinal striations along the axis of extrusion as well as specks <1 μm deep. No evidence of features associated with surface degradation was observed, such as flaking, peeling, or pitting. (B) SEM images of TTV, ADV, and LYNX meshes incubated in oxidative medium for 5 weeks. Low-magnification (40–60 \times , top row) images show the knitted monofilament structure. Medium-magnification (800–1000 \times , middle row) images revealed evidence of pits (black arrows), peeling flakes (double white arrows), and shallow craters (white arrows) on the surface. High-magnification (1500–2000 \times , bottom row) images showed small pits <5 μm in diameter and >1 μm deep on the surface of the mesh for all regions examined. Some regions of the mesh showed evidence of larger scale features, such as detachment of peeling flakes >10 μm long (double white arrows) from the surface, resulting in the formation of shallow craters >10 μm long (white arrows).

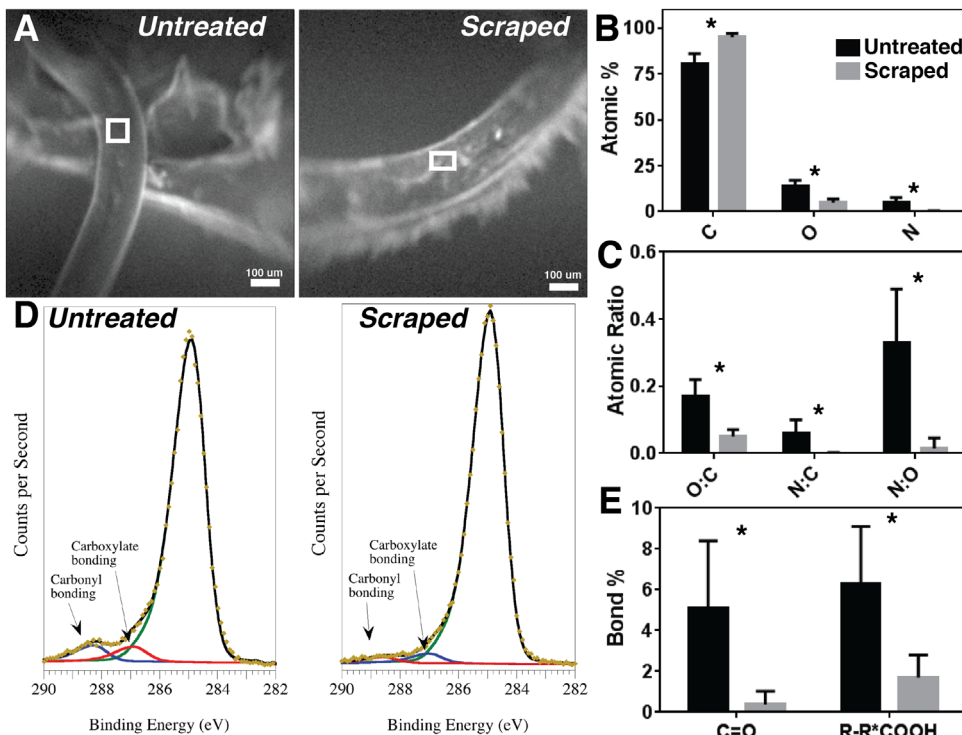


Figure 4. *In vivo* oxidation of explanted PP mesh fibers assessed by XPS. Five explanted Untreated and five Scraped fibers were analysed by XPS to assess the surface concentration of carbon, oxygen, and nitrogen atoms and C1s bonding configurations. One-way ANOVA with Tukey's HSC test for pairwise interactions showed no significant differences between residue-free and residue-present Areas of Interest (AOI) on Untreated fibers, so only Untreated residue-free fibers are shown. Both residue-free and residue-present AOIs on Untreated fibers were significantly different from Scraped fibers. (A) X-ray induced SEM showing the AOI analyzed for a representative sample. (B) Average atomic-% of C, O, and N for the AOI analyzed for each fiber. (C) Average O:C, N:C, and N:O ratios measured for each AOI. (D) High-resolution C1s spectra from Untreated and Scraped fibers. (E) Percent of C1s bonding configurations present on Untreated and Scraped fibers. The complete set of XPS data are shown in the Supplemental Data.

Note: *Denotes statistical significance ($p < 0.05$).

We observed significant increases in carbonyl and hydroxyl peak areas for each mesh after 5 weeks' incubation time in oxidative media by FTIR spectroscopy. In contrast to pristine mesh, which showed longitudinal striations and specks resulting from the extrusion process, SEM images of PP mesh samples at 5 weeks revealed evidence of large-scale pitting, flaking, and peeling associated with surface degradation. Analysis of fibers recovered from an explanted PP mesh by XPS also showed evidence of oxidation *in vivo*. These observations suggest that antioxidants added to PP mesh to protect it during processing and long-term storage do not prevent eventual oxidation in response to ROS, such as hydroxyl radicals present in the oxidative medium (Figure 1), which recapitulates the *in vivo* microenvironment. Thus, antioxidants do not protect the mesh against *in vivo* oxidation and degradation indefinitely.

PP is highly susceptible to oxidation due to its chemical structure, and the mechanism of PP oxidation at elevated temperatures *in vitro* has been known since the 1960s [3,16,25].

However, the effectiveness of antioxidants designed to protect PP against thermal oxidation [25,26] has not been systematically investigated under *in vivo* conditions. Considering recent studies reporting that the body's response to TVM is pro-inflammatory and persists for many years after implantation [8–10,21], the effects of ROS secreted by adherent inflammatory cells on PP should be considered in the design of TVM implants. We investigated oxidation of TVM using a synthetic medium known to recapitulate the oxidative microenvironment between an adherent macrophage and the biomaterial surface [17,18]. This approach enables the investigation of oxidation of PP fibers without the potentially confounding effects of protein adsorption that occurs *in vivo*. Thus, the significant increase in carbonyl and hydroxyl peaks at week 5 (Figure 2) can be explained by oxidation of the PP resulting from the reaction with hydroxyl radicals (Figure 1). Recent attempts to explain the presence of carbonyl peaks on the surface of explanted PP fibers as a crosslinked protein-formalin complex [27], biofilms [28], or residual antioxidants [27] cannot account for the increase in carbonyl and hydroperoxide groups observed after *in vitro* incubation in oxidative medium in the absence of proteins.

Our *in vitro* findings are consistent with previous studies reporting that PP oxidizes *in vivo* [9,12,13,29,30]. In an early study, stabilized PP fibers were solvent-extracted to remove the antioxidant. Extracted PP fibers (which contained a trace of residual antioxidants) and stabilized PP fibers were implanted subcutaneously in hamsters. Extracted PP fibers showed significant oxidation at 108 days, but stabilized PP fibers did not [13]. Thus, the question of whether stabilized PP can oxidize *in vivo* remained unanswered due to insufficient study duration (5 months). In a later study, Prolene® (Ethicon) monofilament PP sutures were implanted in a canine thoracoabdominal bypass model for up to 2 years [30]. Carbonyl absorbance of explanted PP sutures measured by FTIR peaked within 1–3 months post-implantation and subsequently decreased to steady-state values for 2 years.

A more recent study examining TVM explanted from 11 patients reported oxidation of PP fibers as evidenced by carbonyl peaks in the FTIR spectrum [12]. Oxidized PP was distinguished from adsorbed proteins using SEM-EDS to identify regions of PP fibers containing oxygen but not nitrogen. Similarly, we characterized the surface of PP fibers recovered from a mesh explanted from a single patient by XPS, a technique that provides quantitative analysis of the atoms and chemical bonds present at the surface. Collagen has atomic ratios N:C = 0.33 and N:O = 0.83 [31], which are 2–5-fold larger than those measured by XPS for Untreated fibers (Figure 4(C)). After scraping, the N:C and N:O ratios significantly decreased. Furthermore, nitrogen was observed on only 1 of the 5 Scraped fibers, while oxygen was observed on all Scraped fibers. Taken together, these observations suggest that both oxidized PP and adsorbed proteins are present on the surface of the Untreated fibers, which is consistent with previous studies reporting that cleaning explanted PP mesh reduces the carbonyl and hydroxyl peak areas [9,27]. Thus, the presence of oxygen (and absence of nitrogen) detected on the surface of explanted PP fibers by SEM-EDS [12] and XPS (Figure 4) cannot be attributed to protein adsorption [27] alone. Both our findings and those from the SEM-EDS analysis of explanted mesh from 11 patients [12] show that oxidation of PP mesh occurs *in vivo*. Additional studies with larger numbers of patients are warranted to investigate how PP oxidation correlates with mesh degradation and complications in humans.

The methods by which explanted samples are prepared for FTIR and XPS analysis can impact the findings. In the present study, fibers were manually dissected to remove adherent



tissue from an explanted mesh that had not been previously fixed in formalin. Other studies have utilized cleaning solutions, including bleach (sodium hypochlorite) [12,32] or enzymatic [30] treatment to remove biological material from explanted PP fibers fixed in formalin. Cleaning explanted biomedical devices with bleach is recommended in ISO 12,891 for removal of biological tissue from ultra-high molecular weight polyethylene, which has a similar chemical composition to PP [12]. Bleach and enzymatic treatment, as well as microscopic dissection, offer the advantage of selectively removing the tissue without disturbing the integrity of the brittle surface layer. A recent study has proposed a new method for cleaning explanted PP pelvic mesh using twelve cycles of bleach, enzymatic, and ultrasonic treatment, which completely removed the brittle surface layer [27]. Explanted PP fibers cleaned using this method showed no evidence of oxygen, prompting the authors to conclude that the PP fibers were not oxidized and that surface layer comprised crosslinked protein alone. However, ultrasonication cannot selectively separate oxidized PP and adsorbed protein, and thus it is likely that the aggressive twelve-cycle cleaning procedure completely removed the mixed layer of adsorbed proteins and oxidized PP. Testing the composition of the cleaning solutions after ultrasonication for oxidized PP is necessary to support the conclusion that the surface layer contains only protein. In the present study, mechanical scraping of PP fibers from a single explant that was not previously fixed in formalin removed adherent tissue without disturbing the underlying layer of oxidized PP. Further studies with larger numbers of specimens are warranted to confirm the utility of this mechanical scraping without formalin fixation cleaning procedure in additional patients.

Implantation of TVM has been associated with chronic inflammation characterized by predominantly M1 macrophages [8–10,21], PP oxidation [9,12,30], and PP degradation [9,10,12,33]. These findings point to an oxidative degradation mechanism comprising the following steps: (1) attachment of inflammatory cells to the PP surface, (2) secretion of ROS near the PP surface, (3) oxidation and embrittlement of PP, and (4) transverse cracking of PP fibers [12]. Using an established *in vitro* assay, we have shown that ROS secreted by adherent inflammatory cells can oxidize PP mesh stabilized by conventional antioxidants. Consistent with the well-known effect of thermal oxidation on PP degradation [3,16], our data highlight the contribution of ROS-mediated PP oxidation to embrittlement and surface degradation. Clinical studies correlating chronic inflammation with PP degradation [9,10] and mesh exposure [8] establish a potential link between oxidative degradation and mesh complications in patients.

The combination of a biomaterial that undergoes oxidative degradation, an oxidative microenvironment (i.e. the adherent macrophage-biomaterial interface), and residual mechanical stress can result in environmental stress cracking (ESC) [17]. As an example, transverse cracks in explanted poly(ether urethane) catheter leads have been attributed to ESC [17,20,22,34], which has been reproduced *in vitro* by treating pre-strained test specimens in oxidative medium [17]. Previous studies have reported transverse cracks in the surface of explanted PP sutures and mesh [9,29,30]. While PP is generally considered resistant to ESC, the embrittlement of PP by oxidative or other chemical degradation is described as corrosion stress cracking (CSC) [35]. Thus, when PP is exposed to strong oxidizing agents (e.g. ROS) and mechanical stress, it can undergo CSC, resulting in acceleration of the degradation process [25,35]. In the present study, we observed oxidation and surface degradation *in vitro* but did not reproduce the transverse cracking observed for explanted PP sutures and mesh *in vivo*, since the samples were not pre-strained [17] prior to incubation

in the oxidative medium. Thus, future studies in which mesh specimens are pre-strained using forces comparable to those applied *in vivo* (5–15 N [36,37]) prior to treatment with oxidative medium are warranted in order to reproduce cracking of PP mesh *in vitro*.

Conclusions

Oxidative degradation of PP pelvic mesh was evidenced by chemical and physical changes under simulated *in vivo* conditions. PP has been known to be highly susceptible to thermal oxidation at elevated temperatures *ex vivo* since the 1960s [3], and cellular mechanisms of oxidation have been suggested since the 1970s [13,38], but the present study is the first to confirm an ROS-mediated mechanism of PP oxidation and degradation. Since most commercial sources of PP use the same types of antioxidants [25], our findings suggest that oxidation would be expected during the lifetime of the device, and thus antioxidants cannot protect the device from degradation indefinitely. These findings underscore the need for further research into the relative contribution of oxidative degradation to complications associated with PP-based POP and SUI devices.

Disclosure statement

Anne D. Talley and Bridget R. Rogers have no conflicts to disclose. Russell F. Dunn is the Owner of Polymer and Chemical Technologies, which sponsored the work. He has also provided opinions for medico-legal cases on matters related to polypropylene mesh. Vladimir Iakovlev and Scott A. Guelcher have provided opinions for medico-legal cases on matters related to polypropylene mesh.

Funding

This work was supported by Polymer and Chemical Technologies, LLC [grant Number VU-1349].

References

- [1] Caquet F, Collinet P, Debodinance P, et al. Safety of trans vaginal mesh procedure: retrospective study of 684 patients. *J Obstet Gynaecol Res.* 2008;34(4):449–456.
- [2] Nilsson CG, Palva K, Aarnio R, et al. Seventeen years' follow-up of the tension-free vaginal tape procedure for female stress urinary incontinence. *Int Urogynecol J.* 2013;24(8):1265–1269.
- [3] Oswald HJ, Turi E. The deterioration of polypropylene by oxidative degradation. *Polym Eng Sci.* 1965 July;5:152–158.
- [4] Deffieux X, de Tayrac R, Huel C, et al. Vaginal mesh erosion after transvaginal repair of cystocele using Gynemesh or Gynemesh-Soft in 138 women: a comparative study. *Int Urogynecol J.* 2007;18(1):73–79.
- [5] Tsui KP, Ng SC, Tee YT, et al. Complications of synthetic graft materials used in suburethral sling procedures. *Int Urogynecol J.* 2005;16(2):165–167.
- [6] Jia X, Glazener C, Mowatt G, et al. Efficacy and safety of using mesh or grafts in surgery for anterior and/or posterior vaginal wall prolapse: systematic review and meta-analysis. *BJOG: An Int J Obstet Gynaecol.* 2008;115(11):1350–1361.
- [7] Feiner B, Jelovsek JE, Maher C. Efficacy and safety of transvaginal mesh kits in the treatment of prolapse of the vaginal apex: a systematic review. *BJOG: An Int J Obstet Gynaecol.* 2009;116(1):15–24.
- [8] Nolfi AL, Brown BN, Liang R, et al. Host response to synthetic mesh in women with mesh complications. *Am J Obstet Gynecol.* 2016;215(2):206.e1–206.e8.

- [9] Clavé A, Yahi H, Hammou JC, et al. Polypropylene as a reinforcement in pelvic surgery is not inert: comparative analysis of 100 explants. *Int Urogynecol J.* 2010;21(3):261–270.
- [10] Iakovlev VV, Guelcher SA, Bendavid R. Degradation of polypropylene *in vivo*: a microscopic analysis of meshes explanted from patients. *J Biomed Mater Res Part B.* 2015. doi: <http://dx.doi.org/10.1002/jbm.b.33502>; PubMed PMID: 26315946.
- [11] Costello CR, Bachman SL, Grant SA, et al. Characterization of heavyweight and lightweight polypropylene prosthetic mesh explants from a single patient. *Surg Innovation.* 2007;14(3):168–176.
- [12] Imel A, Malmgren T, Dadmun M, et al. *In vivo* oxidative degradation of polypropylene pelvic mesh. *Biomaterials.* 2015;73:131–141.
- [13] Liebert TC, Chartoff RP, Cosgrove SL. Subcutaneous implants of polypropylene filaments. *J Biomed Mater Res.* 1976;10:939–951.
- [14] Kausch HH. The effect of degradation and stabilization on the mechanical properties of polymers using polypropylene blends as the main example. *Macromol Symp.* 2005;225:165–178.
- [15] Hoff A, Jacobsson S. Thermal oxidation of polypropylene in the temperature range of 120–280°C. *J Appl Polym Sci.* 1984;29:465–480.
- [16] Fayolle B, Audouin L, Verdu J. Oxidation induced embrittlement in polypropylene – a tensile testing study. *Polym Degrad Stab.* 2000;70:333–340.
- [17] Zhao QH, McNally AK, Rubin KR, et al. Human plasma alpha2-macroglobulin promotes *in vitro* oxidative stress cracking of Pellethane 2363-80A: *in vivo* and *in vitro* correlations. *J Biomed Mater Res.* 1993;27:379–388.
- [18] Hafeman AE, Zienkiewicz KJ, Zachman AL, et al. Characterization of the degradation mechanisms of lysine-derived aliphatic poly(ester urethane) scaffolds. *Biomaterials.* 2011;32(2):419–429.
- [19] Martin JR, Gupta MK, Page JM, et al. A porous tissue engineering scaffold selectively degraded by cell-generated reactive oxygen species. *Biomaterials.* 2014;35(12):3766–3776.
- [20] Anderson JM, Rodriguez A, Chang DT. Foreign body reaction to biomaterials. *Semin Immunol.* 2008;20:86–100.
- [21] Brown BN, Mani D, Nolfi AL, et al. Characterization of the host inflammatory response following implantation of prolapse mesh in rhesus macaque. *Am J Obstet Gynecol.* 2015;213(5):668.e1–668.e10.
- [22] Schubert MA, Wiggins MJ, Anderson JM, et al. Role of oxygen in biodegradation of poly(etherurethane urea) elastomers. *J Biomed Mater Res.* 1997;34(4):519–530.
- [23] Christenson EM, Anderson JM, Hiltner A. Oxidative mechanisms of poly(carbonate urethane) and poly(ether urethane) biodegradation: *in vivo* and *in vitro* correlations. *J Biomed Mater Res.* 2004;70A(2):245–255.
- [24] Beamson G, Briggs D. High resolution XPS of organic polymers. Chichester, UK: Wiley; 1992.
- [25] Maier C, Calafut T. Polypropylene: the definitive user's guide and databook. New York (NY): William Andrew; 1998.
- [26] de la Rie ER. Polymer stabilizers. A survey with reference to possible applications in the conservation field. *Stud Conserv.* 1988;33:9–22.
- [27] Ong KL, White J, Thamés SF. The myth: *in vivo* degradation of polypropylene meshes. In *Urogynecol J.* 2016;27(Suppl 1):S37–S38.
- [28] de Tayrac R, Letouzey V. Basic science and clinical aspects of mesh infection in pelvic floor reconstructive surgery. *Int Urogynecol J.* 2011;22(7):775–780.
- [29] Costello CR, Bachman SL, Ramshaw BJ, et al. Materials characterization of explanted polypropylene hernia meshes. *J Biomed Mater Res Part B.* 2007;83B(1):44–49.
- [30] Mary C, Marois Y, King MW, et al. Comparison of the *in vivo* behavior of polyvinylidene fluoride and polypropylene sutures used in vascular surgery. *ASAIO J.* 1998;44(3):199–206.
- [31] Szpak P. Fish bone chemistry and ultrastructure: implications for taphonomy and stable isotope analysis. *J Archaeol Sci.* 2011;38:3358072.
- [32] Coda A, Bendavid R, Botto-Micca F, et al. Structural alterations of prosthetic meshes in humans. *Hernia.* 2003;7(1):29–34.
- [33] Gopal S, Majumder S, Batchelor AG, et al. Fix and flap: the radical orthopaedic and plastic treatment of severe open fractures of the tibia. *J Bone Jt Surg.* 2000;82(7):959–966.

- [34] Zhao Q, Agger MP, Fitzpatrick M, et al. Cellular interactions with biomaterials: *in vivo* cracking of pre-stressed pellethane 2363-80A. *J Biomed Mater Res.* 1990;24(5):621–637.
- [35] Chatten R, Vesely D. Environmental stress cracking of polypropylene. In: Karger-Kocsis J, editor. *Polypropylene: an A-Z reference*. Dordrecht: Kluwer Publishers; 1999. p. 206–214.
- [36] Moalli PA, Papas N, Menefee S, et al. Tensile properties of five commonly used mid-urethral slings relative to the TVT. *Int Urogynecol J.* 2008;19(5):655–663.
- [37] Dietz HP, Vancaille P, Svehla M, et al. Mechanical properties of urogynecologic implant materials. *Int Urogynecol J Pelvic Floor Dysfunction.* 2003;14(4):239–243; discussion 43.
- [38] Williams DF. Biodegradation of surgical polymers. *J Mater Sci.* 1982;17:1233–1246.